

# Takahasi Nearest-Neighbour Gas Revisited II: Morse Gases

Akira Matsumoto

Department of Molecular Sciences, Faculty of Science, Osaka Prefecture University, Gakuencho  
1-1, Nakaku, Sakai, Osaka, 599-8531, Japan

Reprint requests to A. M.; E-mail: [akibohn@nifty.com](mailto:akibohn@nifty.com)

Z. Naturforsch. **66a**, 774–778 (2011) / DOI: 10.5560/ZNA.2011-0042

Received April 28, 2011 / revised July 13, 2011

Some thermodynamic quantities for the Morse potential are analytically evaluated at an isobaric process. The parameters of Morse gases for 21 substances are obtained by the second virial coefficient data and the spectroscopic data of diatomic molecules. Also some thermodynamic quantities for water are calculated numerically and drawn graphically. The inflexion point of the length  $L$  which depends on temperature  $T$  and pressure  $P$  corresponds physically to a boiling point.  $L$  indicates the liquid phase from lower temperature to the inflexion point and the gaseous phase from the inflexion point to higher temperature. The boiling temperatures indicate reasonable values compared with experimental data. The behaviour of  $L$  suggests a chance of a first-order phase transition in one dimension.

*Key words:* Takahasi Nearest-Neighbour Gas; Morse Potential; Boiling Temperature; Equation of State; Enthalpy; First-Order Phase Transition.

## 1. Introduction

In the previous paper the behaviour of the length  $L$  has given a chance of a first-order phase transition in one dimension [1] while Takahasi had pointed out that the coexistence of two phases is impossible in a one-dimensional substance for any choice of the potential [2]. On one hand, the Morse potential has been applied to the intermolecular potential as the van der Waals force in atomic collision [3], and the parameters of the Morse potential have been derived from the second virial coefficients [4]. It is especially interesting that the Morse potential is able to be applied to polar molecules which consist of the electrostatic interaction of two dipoles.

In this work, the parameters for Morse gases are obtained by the second virial coefficients and the spectroscopic data of diatomic molecules. The length  $L$ ,  $(dL/dT)_P$ , enthalpy, and heat capacity are analytically represented of the two intensive variables  $T$  and  $P$ . These thermodynamic quantities are determined through numerical calculations, and are graphically displayed at atmospheric pressure for  $H_2O$ . The chance of the first-order phase transition for the Morse potential at boiling points and atmospheric pressure is discussed.

## 2. Thermodynamic Functions of Morse Gases at the Isobaric Process

The particles and the gas constants in one dimension are calculated as follows [1, 5]. The number of particles obtained is

$$N_1 = 0.84446 \cdot 10^8, \quad (1)$$

and consequently, a gas constant is

$$R_1 = kN_1 = 1.1659 \cdot 10^{-15} \text{ J K}^{-1}. \quad (2)$$

Another gas constant per particle corresponds to

$$k_1 = 0.122233 \text{ atm \AA K}^{-1} \quad (3)$$

and therefore

$$R_1 = k_1 N_1 = 0.103221 \text{ atm cm K}^{-1}. \quad (4)$$

The Morse potential is expressed as

$$U(r) = D \exp[-2\alpha(r - r_e)] - 2D \exp[-\alpha(r - r_e)]. \quad (5)$$

Introducing the new variables

$$u = \beta D, \quad (6)$$

where  $\beta = 1/kT$ ,

$$x = u \exp[-2\alpha(r - r_e)], \tag{7}$$

$$r = (\log x_0 - \log x)/2\alpha, \tag{8}$$

$$\log x_0 = 2\alpha r_e + \log u, \tag{9}$$

$$q = \beta P/2\alpha, \tag{10}$$

and

$$f(x) = x - 2\sqrt{ux}. \tag{11}$$

Then, the configurational partition function for the Morse potential may be defined as

$$Q_0 = \frac{1}{2\alpha x_0^q} \int_0^\infty \exp[-f(x)]x^{q-1} dx \tag{12}$$

and

$$Q = \frac{1}{x_0^q} \int_0^\infty \exp[-f(x)]x^{q-1} dx. \tag{13}$$

The partition function in the  $T$ - $P$  grand canonical ensemble is expressed as the product of kinetic and configurational partition functions,

$$Y(T, P, N_1) = \left(\frac{2\pi mkT}{h^2}\right)^{N_1/2} Q_0(T, P)^{N_1}. \tag{14}$$

The Gibbs free energy is derived from (14) as

$$G(T, P) = -N_1 kT \left[ \log \frac{(2\pi mkT)^{1/2}}{h} - \log 2\alpha + \log Q(T, P) \right]. \tag{15}$$

The equation of state in one dimension is expressed as

$$L = \left(\frac{\partial G}{\partial P}\right)_T = \frac{R_1 T}{P} \frac{1}{Q x_0^q} \int_0^\infty qX \exp[-f(x)]x^{q-1} dx, \tag{16}$$

where

$$X = \log x_0 - \log x. \tag{17}$$

The derivative of  $L$  with respect to  $T$  can be derived from (16):

$$\left(\frac{\partial L}{\partial T}\right)_P = \frac{R_1}{P} \left[ \frac{1}{Q x_0^q} \int_0^\infty qX [f(x) + qX] \exp[-f(x)] \cdot x^{q-1} dx - \frac{1}{Q^2 x_0^{2q}} \int_0^\infty qX \exp[-f(x)]x^{q-1} dx \cdot \int_0^\infty [f(x) + qX] \exp[-f(x)]x^{q-1} dx \right]. \tag{18}$$

The enthalpy is obtained as

$$H = -T^2 \left[ \frac{\partial}{\partial T} \left( \frac{G}{T} \right) \right]_P = R_1 T \left[ \frac{1}{2} + \frac{1}{Q x_0^q} \int_0^\infty [f(x) + qX] \exp[-f(x)]x^{q-1} dx \right]. \tag{19}$$

The heat capacity at constant pressure can be easily derived from (18):

$$C_P = \left(\frac{\partial H}{\partial T}\right)_P = R_1 \left[ \frac{1}{2} + \frac{1}{Q x_0^q} \int_0^\infty [f(x) + qX]^2 \exp[-f(x)]x^{q-1} dx - \frac{1}{Q x_0^{2q}} \left\{ \int_0^\infty [f(x) + qX] \exp[-f(x)]x^{q-1} dx \right\}^2 \right]. \tag{20}$$

The integrals which are contained in (13), (16), (18), (19), and (20) can be explicitly calculated as follows:

$$\int_0^\infty \exp[-x+2\sqrt{ux}]x^{a-1} dx = \Gamma(a) \sum_{n=0}^\infty \frac{(a)_n u^n}{(1/2)_n n!} + 2\sqrt{u} \Gamma(a+1/2) \sum_{n=0}^\infty \frac{(a+1/2)_n u^n}{(3/2)_n n!}, \tag{21}$$

$$\int_0^\infty \exp[-x+2\sqrt{ux}]x^{a-1} (\log x) dx = \Gamma(a) \sum_{n=0}^\infty \frac{(a)_n \psi(n+a) u^n}{(1/2)_n n!} + 2\sqrt{u} \Gamma(a+1/2) \sum_{n=0}^\infty \frac{(a+1/2)_n \psi(n+a+1/2) u^n}{(3/2)_n n!}, \tag{22}$$

and

$$\int_0^\infty \exp[-x+2\sqrt{ux}]x^{a-1} (\log x)^2 dx = \Gamma(a) \sum_{n=0}^\infty \frac{(a)_n [\psi^2(n+a) + \psi^{(1)}(n+a)] u^n}{(1/2)_n n!} + 2\sqrt{u} \Gamma(a+1/2) \sum_{n=0}^\infty \frac{(a+1/2)_n [\psi^2(n+a+1/2) + \psi^{(1)}(n+a+1/2)] u^n}{(3/2)_n n!}, \tag{23}$$

where the polygamma function  $\psi(x)$  is defined as

$$\psi(x) = \frac{d \log \Gamma(x)}{dx} = \frac{\Gamma'(x)}{\Gamma(x)} \quad (24)$$

and

$$\psi^{(n)}(x) = \frac{d^n \psi(x)}{dx^n}. \quad (25)$$

The second virial coefficients for the intermolecular potential  $U(r)$  may be found, for classical statistics, from the well-known formula

$$B(T) = -\frac{2\pi N_A}{3} \int_0^\infty \beta \frac{dU(r)}{dr} \exp[-\beta U(r)] r^3 dr, \quad (26)$$

where  $N_A$  is the Avogadro number. The second virial coefficients for Morse gases [4] are expressed as

$$\begin{aligned} B(T) &= -\frac{\pi N_A}{12\alpha^3} \int_0^\infty \exp[-x + 2\sqrt{ux}](x - \sqrt{ux}) \\ &\quad \cdot X^3 x^{-1} dx, \\ &= -\frac{\pi N_A}{4\alpha^3} \left[ \sqrt{\pi u} \sum_{n=0}^\infty \frac{u^n}{n!} g(n+1/2, x_0) \right. \\ &\quad \left. + \sum_{n=1}^\infty \frac{u^n}{(1/2)_n} g(n, x_0) + \frac{1}{3} h(1, x_0) \right], \end{aligned} \quad (27)$$

where

$$\begin{aligned} h(z, x_0) &= [\psi(z) - \log x_0]^3 \\ &\quad + 3[\psi(z) - \log x_0] \psi^{(1)}(z) + \psi^{(2)}(z) \end{aligned} \quad (29)$$

and

$$g(z, x_0) = \frac{1}{z} [\{\psi(z) - \log x_0\}^2 + \psi^{(1)}(z)]. \quad (30)$$

### 3. Numerical Results

The parameters of the Morse potential for 17 substances in A and B,  $D$ ,  $r_e$ , and  $\alpha$  are determined from the experimental data of the second virial coefficients [6] and those for eight substances in C are derived from the spectroscopic data [7] as shown in Table 1. Eigenvalues of the Morse potential due to the anharmonic oscillator [4] are represented as

Table 1. Parameters for Morse gas: Substances in part A and B are determined from experimental data of the second virial coefficients [6]. Those in part C are derived from spectroscopic data of diatomic molecules [7].

Substance	$(D/k)/K$	$r_e/\text{\AA}$	$\alpha/\text{\AA}^{-1}$
A			
Ne	44.319	2.91	1.87707
Ar	122.539	4.05	1.27667
Kr	188.791	4.12	1.31562
Xe	225.900	4.79	1.09181
N <sub>2</sub>	95.990	4.42	1.18689
O <sub>2</sub>	158.646	3.72	1.60520
F <sub>2</sub>	117.812	4.39	1.25105
CO	102.118	4.48	1.17042
CH <sub>4</sub>	151.846	4.46	1.17591
B			
HCl	654.829	2.71	2.24844
H <sub>2</sub> O	1984.89	2.60	5.92827
SO <sub>2</sub>	1016.76	2.72	2.33451
NH <sub>3</sub>	1020.40	2.62	3.27677
CH <sub>3</sub> F	769.467	3.26	2.83133
CH <sub>3</sub> Cl	1168.32	3.14	3.56828
CH <sub>3</sub> OH	1545.10	2.53	3.28000
CH <sub>3</sub> NH <sub>2</sub>	1032.32	2.69	2.03723
C			
Ne	33.297	3.15	1.09650
Ar	140.480	3.7580	1.41806
Kr	199.046	4.030	1.61624
Xe	281.863	4.3610	1.48370
K	6030.81	3.9051	0.76398
Rb	5727.40	4.06	0.72076
Cs	4602.37	4.470	0.73759
Al	18238.0	2.4660	1.39053

$$\begin{aligned} E_n &= -D + \frac{\alpha h}{\pi} \sqrt{\frac{D}{2\mu}} (n + 1/2) \\ &\quad - \frac{\alpha^2 h}{8\pi^2 \mu} (n + 1/2)^2. \end{aligned} \quad (31)$$

Another value is given by the spectroscopic constants

$$E_n = -D + \omega_e(n + 1/2) - \omega_e x_e(n + 1/2)^2. \quad (32)$$

The dissociation energy  $D_0$  is

$$D_0 = -E_0 = D - \omega_e/2 + \omega_e x_e/4, \quad (33)$$

where  $D$  is the energy depths and  $\mu$  the reduced mass. The parameter  $\alpha$  has the relation

$$\frac{\alpha h}{\pi} \sqrt{\frac{D}{2\mu}} = \omega_e. \quad (34)$$

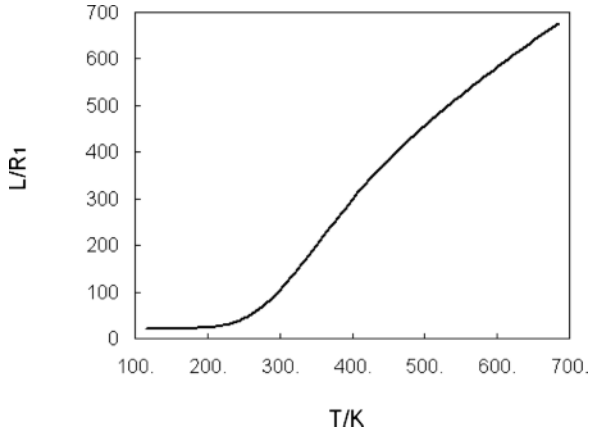


Fig. 1. Length  $L$  for  $H_2O$  vs. temperature at  $P = 1$  atm,  $T_B = 349$  K.

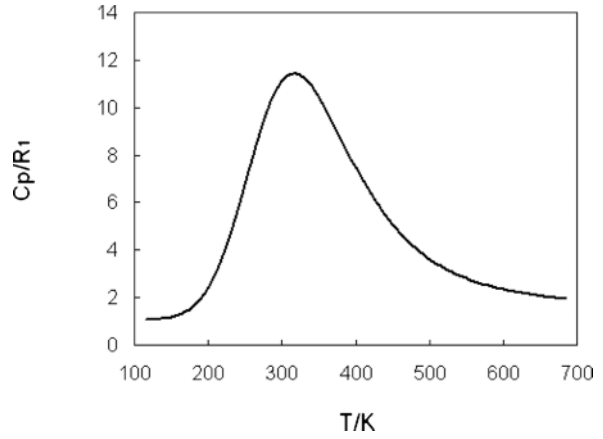


Fig. 4. Heat capacity  $C_p$  for  $H_2O$  vs. temperature at  $P = 1$  atm,  $T_B = 349$  K.

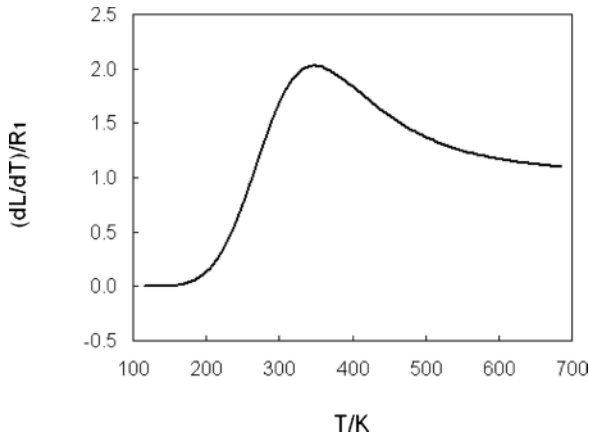


Fig. 2. Derivative  $(dL/dT)_P$  for  $H_2O$  vs. temperature at  $P = 1$  atm,  $T_B = 349$  K.

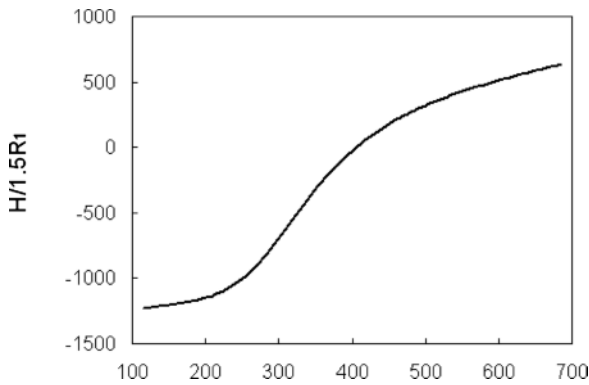


Fig. 3. Enthalpy  $H$  for  $H_2O$  vs. temperature at  $P = 1$  atm,  $T_B = 349$  K.

Table 2.  $T_1$  (temperature for maximum of  $C_p$ ) and boiling temperature  $T_B$  for different substances at 1 atm.

Substance	Morse gas		Exp. result [11] $T_B/K$
	$T_1/K$	$T_B/K$	
<i>A</i>			
Ne	22	36	27.0
Ar	47	72	87.3
Kr	63	90	119.8
Xe	76	108	165.0
$N_2$	41	66	77.4
$O_2$	53	75	90.2
$F_2$	46	71	85.0
CO	43	68	81.7
$CH_4$	56	83	111.7
<i>B</i>			
HCl	146	176	188.1
$H_2O$	317	349	373.2
$SO_2$	208	243	263
$NH_3$	197	227	239.7
$CH_3F$	160	188	194.8
$CH_3Cl$	218	248	248.9
$CH_3OH$	280	316	337.8
$CH_3NH_2$	216	254	266.8
<i>C</i>			
Ne	25	49	27.0
Ar	51	73	87.3
Kr	62	85	119.8
Xe	82	110	165.0
K	1107	1252	1027.0
Rb	1070	1207	952
Cs	888	1051	951.6
Al	2631	2834	2766.8

The Morse potential in A and B consists in the quantum-mechanical vibrational levels.

Numerical results obtained with the length  $L$ ,  $(dL/dT)_P$ , enthalpy, and heat capacity for  $H_2O$  at atmospheric pressure are displayed in Figures 1–4. As shown in Figure 2, the curve of  $(dL/dT)_P$  in (21) has a maximum at the temperature  $T_2$  which is the inflexion point of the length  $L$ . This curve of  $(dL/dT)_P$  may reach asymptotically to 0 with decreasing  $T$  and to 1 with increasing  $T$  beyond  $T_2$ . Considering Figure 2, the curve of  $L$  in Figure 1 is definitely away from  $T_2$  and the behaviours of ideal gases. Also, similar to  $(dL/dT)_P$ , the curve of the heat capacity in Figure 4 shows a maximum at the temperature  $T_1$  which is the inflexion point of the enthalpy  $H$ . The enthalpy reaches the behaviour of ideal gases at higher temperature beyond  $T_1$ . The heat capacity becomes asymptotically  $1.5 R_1$  at higher temperature than  $T_1$ .  $(dL/dT)_P$  and  $C_P$  are originally not maxima but must diverge to infinite according to three-dimensional models [8–10]. This point of  $L$ , however, corresponds physically to

a boiling point, while  $L$  does not show a sudden change but a sluggish one in the neighbourhood of the inflexion point  $T_2$ .  $L$  in Figure 1 indicates the liquid phase from lower temperature to the inflexion point and the gaseous phase from the inflexion point to higher temperature. The Morse potential for polar gases in B seem especially to include a factor of the long-range interaction which consists of the electrostatic dipole–dipole function [1].

In one dimension, the inflexion point of  $L$  does not agree with that of  $H$  though a jump for  $H$  is graphically observed from the liquid to the gaseous phase at the boundary of the boiling point in the three-dimensional models [8–10]. Assuming that boiling temperature  $T_B$  is physically equivalent to the inflexion point of  $L$ ,  $T_2$ , the boiling temperatures for polar substances indicate reasonable values compared with experimental data [11] as shown in Table 2. The behaviour of  $(dL/dT)_P$  in the neighbourhood of the boiling point corresponds to a first-order phase transition in one dimension.

- [1] A. Matsumoto, *Z. Naturforsch.* **66a**, 247 (2011).
- [2] H. Takahasi, *Proc. Phys. Math. Soc. Japan* **24**, 60 (1942).
- [3] K. Fuke, T. Saito, and K. Kaya, *J. Chem. Phys.* **81**, 2591 (1984).
- [4] A. Matsumoto, *Z. Naturforsch.* **42a**, 447 (1987).
- [5] T. Nagamiya, *Proc. Phys. Math. Soc. Japan* **22**, 705 (1940).
- [6] J. H. Dymond and E. B. Smith, *The Virial Coefficients of Pure Gases and Mixtures*, Clarendon Press, Oxford 1980.
- [7] H. Huber and G. Herzberg, *Molecular Spectra and Molecular Structure VI, Constants of Diatomic Molecules*, van Nostrand Reinhold, New York 1977.
- [8] A. Matsumoto, *Z. Naturforsch.* **60a**, 783 (2005).
- [9] A. Matsumoto, *Z. Naturforsch.* **65a**, 561 (2010).
- [10] P. W. Atkins, *Physical Chemistry*, 6th Edn., Oxford University, Oxford 1998, p. 153.
- [11] R. C. Reid, J. M. Prausnitz, and T. K. Sherwood, *The Properties of Gases and Liquids*, 3rd Edn., Appendix A, McGraw–Hill, New York, 1977.